RSC Advances

PAPER

View Article Online
View Journal | View Issue

Cite this: *RSC Adv.*, 2021, **11**, 30465

Revealing photoluminescence mechanisms of single $CsPbBr_3/Cs_4PbBr_6$ core/shell perovskite nanocrystals†

Huafeng Ding,‡[a] Yansu Shan,‡[a] Jizhou Wang,‡[b] Qinfeng Xu,*[a] Jing Han,[a] Mengmeng Jiao,[a] Kunjian Cao,[a] Mingliang Liu,[a] Haifeng Mu,*[a] Shufang Zhang[a] and Chuanlu Yang*[a]

$CsPbBr_3$ nanocrystals (NCs) encapsulated by Cs_4PbBr_6 has attracted extensive attention due to good stability and high photoluminescence (PL) emission efficiency. However, the origin of photoluminescence (PL) emission from $CsPbBr_3/Cs_4PbBr_6$ composite materials has been controversial. In this work, we prepare $CsPbBr_3/Cs_4PbBr_6$ core/shell nanoparticles and firstly study the mechanism of its photoluminescence (PL) at the single-particle level. Based on photoluminescence (PL) intensity trajectories and photon antibunching measurements, we have found that photoluminescence (PL) intensity trajectories of individual $CsPbBr_3/Cs_4PbBr_6$ core/shell NCs vary from the uniform longer periods to multiple-step intensity behaviors with increasing excitation level. Meanwhile, second-order photon correlation functions exhibit single photon emission behaviors especially at lower excitation levels. However, the PL intensity trajectories of individual Cs_4PbBr_6 NCs demonstrate apparent "burst-like" behaviors with very high values of $g^2(0)$ at any excitation power. Therefore, the distinguishable emission statistics help us to elucidate whether the photoluminescence (PL) emission of $CsPbBr_3/Cs_4PbBr_6$ core/shell NCs stems from band-edge exciton recombination of $CsPbBr_3$ NCs or intrinsic Br vacancy states of Cs_4PbBr_6 NCs. These findings provide key information about the origin of emission in $CsPbBr_3/Cs_4PbBr_6$ core/shell nanoparticles, which improves their utilization in the further optoelectronic applications.

Received 28th June 2021
Accepted 12th August 2021

DOI: 10.1039/d1ra04981j

rsc.li/rsc-advances

1. Introduction

All-inorganic perovskite nanocrystals (NCs) have received extensive attention in solar cell and light-emitting devices due to their facile synthesis[1–3] and excellent photophysical properties such as high photoluminescence quantum yields (PLQYs),[4] narrow emission width,[5,6] and tunable emission features that cover the full visible range.[7,8] As a result, they have shown promising applications in optoelectronics, including photovoltaics,[9,10] lasing,[11,12] light-emitting diodes[13–15] and photodetectors.[16,17] However, the photoluminescence quantum yields (PLQYs) of $CsPbX_3$ NCs are greatly reduced when they are in the form of agglomerates compared to well-dispersed colloidal NCs.[18] At present, an effective approach to solve these problems is to modify the surface structures of $CsPbX_3$ NCs and alleviate the stability.[19,20] $CsPbX_3$ perovskite NCs coated with heterostructure shell have been reported, such as $CsPbX_3$/ZnS core/shell NCs,[21] $CsPbBr_3/SiO_2$ and $CsPbBr_3/Ta_2O_5$.[22] Recently, it is unsurprising that Cs_4PbBr_6 lattice spacing could match the cubic $CsPbBr_3$ lattice constants and this match satisfies the $CsPbBr_3$ NCs inside the Cs_4PbBr_6 matrix, with enhanced passivation of the surfaces without additional strain on the NCs. Therefore, $CsPbBr_3$ coated with the same chemical constituents Cs_4PbBr_6 has been proven to be an effective way to maintain the highly efficient photoluminescence quantum yields (PLQYs) and simultaneously improve the stabilities.[23,24]

Despite the synthesis of $CsPbBr_3$ perovskite NCs encapsulated by Cs_4PbBr_6 material enables high emission efficiency and excellent stability, the photoluminescence origin of $CsPbBr_3/Cs_4PbBr_6$ core/shell perovskite NCs have attracted a lot of attention as well as intensive debates. The debates on the origin of bright photoluminescence emission involve two opposing opinions. Due to the extreme similarity of its photoluminescence emission with that of $CsPbBr_3$ nanocrystals, it is believed encapsulated $CsPbBr_3$ nanocrystals are responsible for the highly efficient photoluminescence.[25–30] However, some researchers have attributed the photoluminescence emission to Br defects in the Cs_4PbBr_6 and regarding the photoluminescence emission as an intrinsic property of Cs_4PbBr_6.[31–36]

[a]*Department of Physics and Optoelectronic Engineering, Ludong University, Yantai 264025, People's Republic of China. E-mail: xuqf5678@163.com; hai-fengmu@163.com; yangchuanlu@126.com*

[b]*Lanzhou Institute of Space Technology and Physics, Lanzhou 730000, People's Republic of China*

† Electronic supplementary information (ESI) available. See DOI: 10.1039/d1ra04981j

‡ H. F. Ding, Y. S. Shan and J. Z. Wang contributed equally to this work.

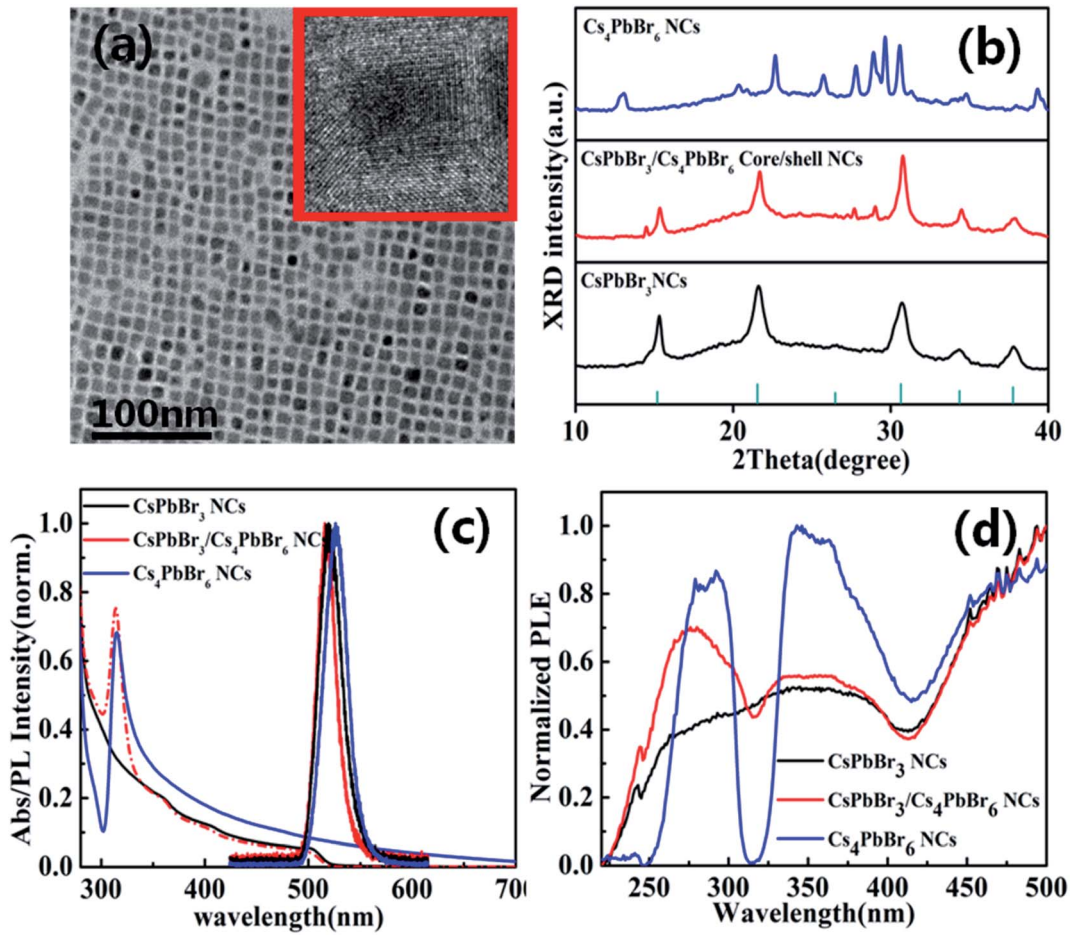

Fig. 1 (a) TEM images of $CsPbBr_3/Cs_4PbBr_6$ core/shell perovskite NCs and corresponding magnified individual core/shell NC (top right corner); (b) XRD patterns of Cs_4PbBr_6 NCs, $CsPbBr_3/Cs_4PbBr_6$ core/shell NCs and $CsPbBr_3$ NCs; (c) absorption and PL spectra of Cs_4PbBr_6, $CsPbBr_3/Cs_4PbBr_6$ core/shell NCs and $CsPbBr_3$ NCs; (d) photoluminescence excitation (PLE) spectra of Cs_4PbBr_6, $CsPbBr_3/Cs_4PbBr_6$ core/shell NCs and $CsPbBr_3$ NCs, the monitored wavelength for PLE is 520 nm and the excitation wavelength for PL is 405 nm.

To fully exploit the origin of their PL emission, it is vital to deeply gain the important information about the interaction with the encapsulating media and complex PL dynamics process. Therefore, studies of the PL properties at the single-particle level has been proved to be a very effective method for elucidate its PL origins.

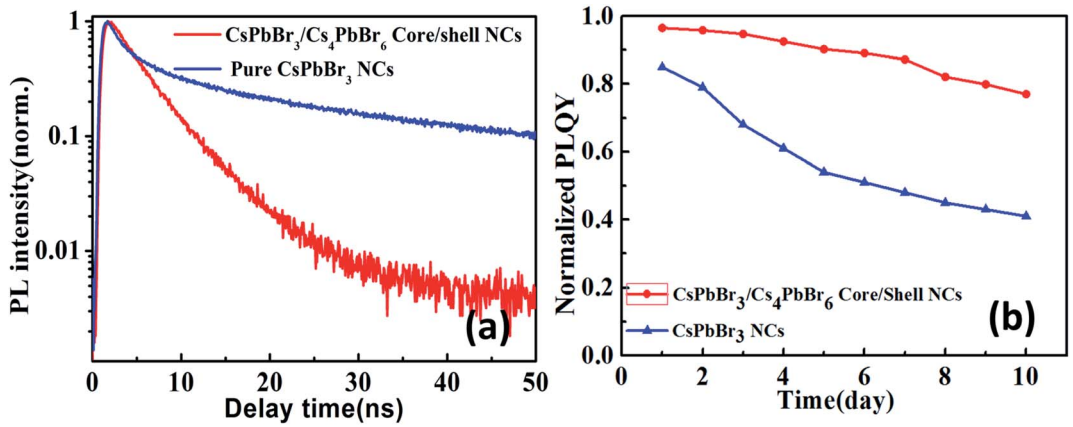

Fig. 2 (a) Time-resolved photoluminescence (TRPL) decays of $CsPbBr_3$ NCs and $CsPbBr_3/Cs_4PbBr_6$ core/shell NCs; (b) PLQYs of $Cs_4PbBr_6/CsPbBr_3$ core/shell NCs and $CsPbBr_3$ NCs exposed to air for different days under ambient conditions.

In this report, we present a simple solution-processed chemical method to synthesize $CsPbBr_3/Cs_4PbBr_6$ core/shell NCs and investigate the PL intensity trajectories from individual $CsPbBr_3/Cs_4PbBr_6$ core/shell NCs and Cs_4PbBr_6 NCs by time-correlated single photon counting (TCSPC). We analyse PL lifetimes and second-order correlation functions $g^2(\tau)$ at different excitation levels in order to explain the origin of their PL emission.

2. Experimental section

The $CsPbBr_3/Cs_4PbBr_6$ core/shell perovskite nanocrystals were synthesized through the hot-injection method with detailed processes presented in ESI.† The resulting $CsPbBr_3$ NCs solution was lowered to room temperature and 0.1 mmol (or 0.2 mmol) $ZnBr_2$ was added to the flash, degassed at 50 °C for 20 min under vacuum. Afterward the temperature was raised to 70 °C under a nitrogen atmosphere, Cs-oleate with different amount (0.203 mmol corresponding to a shell thickness of 1.5 nm) was quickly injected. The solution was lowered to room temperature using a water bath after 3 min. The solution turned bright green again. To collect the NCs, the crude solution was then centrifuged at 8000 rpm for 5 min. After centrifugation, the supernatant was discarded and the $CsPbBr_3/Cs_4PbBr_6$ core/shell NCs were prepared.

For the single-dot measurements, $CsPbBr_3/Cs_4PbBr_6$ core/shell NCs solution diluted in toluene has been mixed with PMMA (5wt%) and spin-coated onto a glass coverslip at the

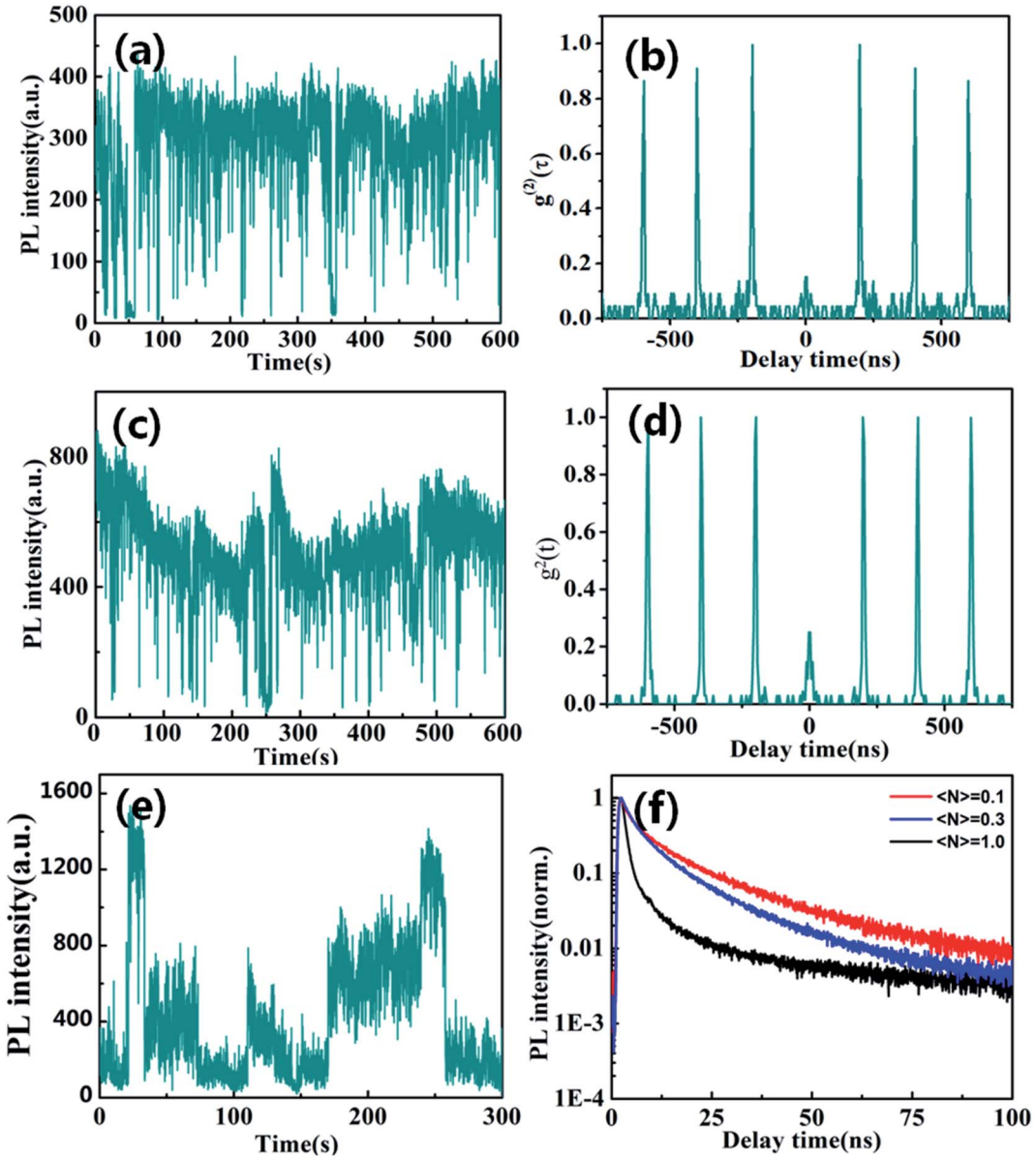

Fig. 3 Blinking trajectories of individual Cs_4PbBr_6 NC at low (a) $\sim\langle N\rangle = 0.1$ and high excitation level (c) $\sim\langle N\rangle = 0.5$, (d) $\sim\langle N\rangle = 1.0$, respectively. Antibunching functions $g^2(t)$ at low (b) $\sim\langle N\rangle = 0.1$ and high (e) $\sim\langle N\rangle = 1$ excitation levels. (f) Corresponding PL lifetimes at different excitation levels.

speed of 3000 rpm. The QDs density was kept below 0.1 μm^{-2} to allow us to probe single QD with detailed processes presented in ESI.†

3. Results and discussion

The $CsPbBr_3/Cs_4PbBr_6$ core/shell perovskite nanocrystals were synthesized through a hot-injection method with detailed processes provided in experimental section (see ESI†). Fig. 1a indicates the TEM image of $CsPbBr_3/Cs_4PbBr_6$ core/shell perovskite NCs. The TEM image of $CsPbBr_3/Cs_4PbBr_6$ core/shell perovskite nanocrystals have a cubic shape and the core $CsPbBr_3$ are coated by Cs_4PbBr_6 shell (inset in Fig. 1a).

To further confirm the formation of $CsPbBr_3/Cs_4PbBr_6$ core/shell NCs, the X-ray diffraction (XRD) spectroscopy was performed as shown in Fig. 1b. The $CsPbBr_3/Cs_4PbBr_6$ core/shell NCs display a combination between the cubic $CsPbBr_3$ phase and hexagonal Cs_4PbBr_6 phase. According to the results from X-ray diffraction spectroscopy (XRD), the main peaks should correspond to the cubic crystal, indicating that the $CsPbBr_3$ still maintain their initial crystal phase. Meanwhile, the minor peaks can be ascribed to hexagonal phase of Cs_4PbBr_6, revealing the formation of Cs_4PbBr_6 shell. Therefore, it implies that the XRD of $CsPbBr_3/Cs_4PbBr_6$ core/shell NCs is different from the simple mixtures of $CsPbBr_3$ and Cs_4PbBr_6 in bulk.

The absorption and PL spectra of the $CsPbBr_3$ NCs, $CsPbBr_3/Cs_4PbBr_6$ core/shell NCs and Cs_4PbBr_6 NCs are presented in Fig. 1c. After the Cs_4PbBr_6 shell encapsulation, it was found that the additional characteristic peaks were located at 315 nm, which can be attributed to the absorption from Cs_4PbBr_6, suggesting the formation of Cs_4PbBr_6 shell structures. The PL peak of Cs_4PbBr_6 perovskite NCs displays an obvious red shift from 515 nm to 520 nm. Fig. 1d shows the Photoluminescence excitation (PLE) spectra of $CsPbBr_3/Cs_4PbBr_6$ core/shell NCs emission at 515 nm. Compared with $CsPbBr_3/Cs_4PbBr_6$ core/shell NCs, the Cs_4PbBr_6 exhibits a obvious sharp dip at the wavelength of 310 nm, where light is fully absorbed by the Cs_4PbBr_6. Therefore, it also demonstrate that $CsPbBr_3/Cs_4PbBr_6$ core/shell NCs is different from Cs_4PbBr_6 NCs.

In order to get deep insights into the carrier dynamics induced by the core/shell structure, we investigate time-resolved photoluminescence (TRPL) decay behavior of $CsPbBr_3/Cs_4PbBr_6$ core/shell NCs as shown in Fig. 2a. The average lifetime of $CsPbBr_3/Cs_4PbBr_6$ core/shell NCs is 7.1 ns, which is much shorter than average lifetime 9.6 ns of pure $CsPbBr_3$ NCs. This could be attribute to the thicker shell structures of Cs_4PbBr_6 that reduce the probability of carriers being captured by the surface traps due to the enhanced overlap of wave functions. According to analysis on absorption spectra, the $CsPbBr_3$ core (2.4 eV, 515 nm) was coated by Cs_4PbBr_6 shell with large band gap (4.0 eV, 310 nm). Therefore, the photogenerated electron and hole will be confined in the core regions. The shell can passivate the surface states of the core and reduce nonradiative recombination pathways. After $CsPbBr_3$ encapsulated with Cs_4PbBr_6 shell, the PLQYs was improved from 83.6% to 96.8% corresponding to a 13% improvement after shell encapsulation. Under the same excitation experimental conditions, the PL peak of $CsPbBr_3/Cs_4PbBr_6$ core/shell NCs remains almost unaltered at 515 nm, showing a robust resistance to anion exchange reaction. Under continuous excitation by 405 nm laser, $CsPbBr_3/Cs_4PbBr_6$ core/shell NCs show a much better stability than colloidal $CsPbBr_3$ NCs. $CsPbBr_3/Cs_4PbBr_6$ core/shell NCs retains about 77% emission intensity after illumination for 10 days and $CsPbBr_3$ NCs retains less than 45% as shown in Fig. 2b, indicating improved PL stability in air compared to the pure $CsPbBr_3$ NCs.

Fluorescence blinking has been extensively investigated in semiconductor nanostructures, providing unique insight into their photo-excited carrier dynamics. Here, we firstly explored blinking trajectories of individual $CsPbBr_3/Cs_4PbBr_6$ core/shell NCs with different excitation level, respectively. Fig. 3a and c present the PL intensity trajectories with obvious on states and gray states under the low excitation level of $\langle N\rangle = 0.1$ and $\langle N\rangle = 0.3$, respectively. Fig. 3b and d show single quantum emitters with low values $g^2(0)<0.5$ corresponding to low excitation level of

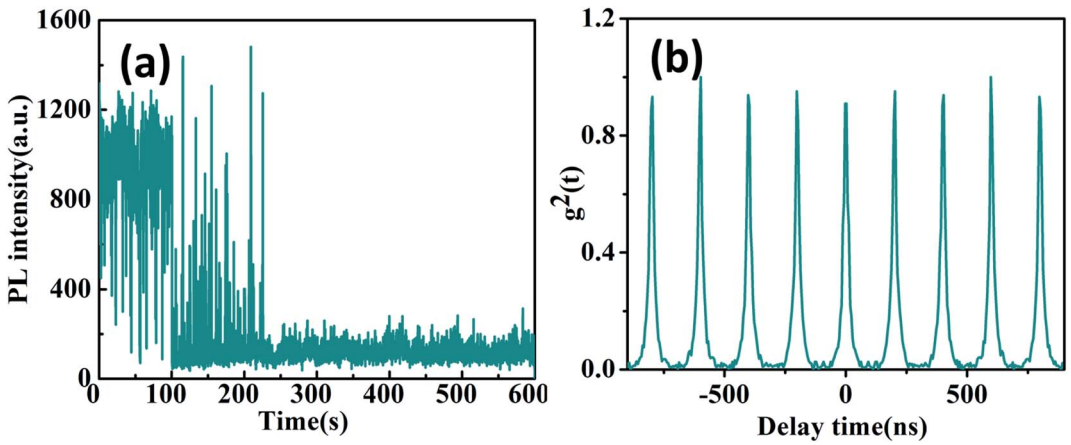

Fig. 4 (a) Blinking trajectories and (b) antibunching functions $g^2(t)$ of individual $CsPbBr_3/Cs_4PbBr_6$ core/shell NC at high excitation level ($\langle N\rangle = 1.3$).

$\langle N\rangle = 0.1$ and $\langle N\rangle = 0.3$, respectively. However, the blinking behavior of the $CsPbBr_3/Cs_4PbBr_6$ NCs visibly changed at high excitation level of $\langle N\rangle = 1.0$. It is clearly seen that blinking trajectories is no longer represented by two-state emission but is multiple-step intensity emission as shown in Fig. 3e. PL lifetimes extracted from different intensity levels are composed of the fast (approximate 1 to 2 ns) and slow (approximate 9 to 10 ns) component with varying amplitudes as shown in Fig. 3f. Longer lifetime components predominate in the higher intensity bursts and the shorter ones in the low intensity intervals correspond to the on and gray states, respectively. The PL lifetime of on state obviously demonstrates the near band edge excitonic transitions. On the contrary, the PL lifetime of the gray state is much shorter and it indicates that the emission is likely coming from a charged excitonic state. These results correspond well with previously measured PL lifetimes for individual $CsPbBr_3$ NCs.[37,38]

When individual $CsPbBr_3/Cs_4PbBr_6$ core/shell NCs was excited with $\langle N\rangle = 1.3$ higher excitation levels for longer times, the blinking trajectories demonstrate a very peculiar emission behavior as shown in Fig. 4a. It starts at the stable intensity level with 1000 to 1200 counts, typical for two state emission. After 100 seconds, the PL intensity starts to exhibit large jumps to the 400 to 1200 counts level. The lifetimes extracted from different

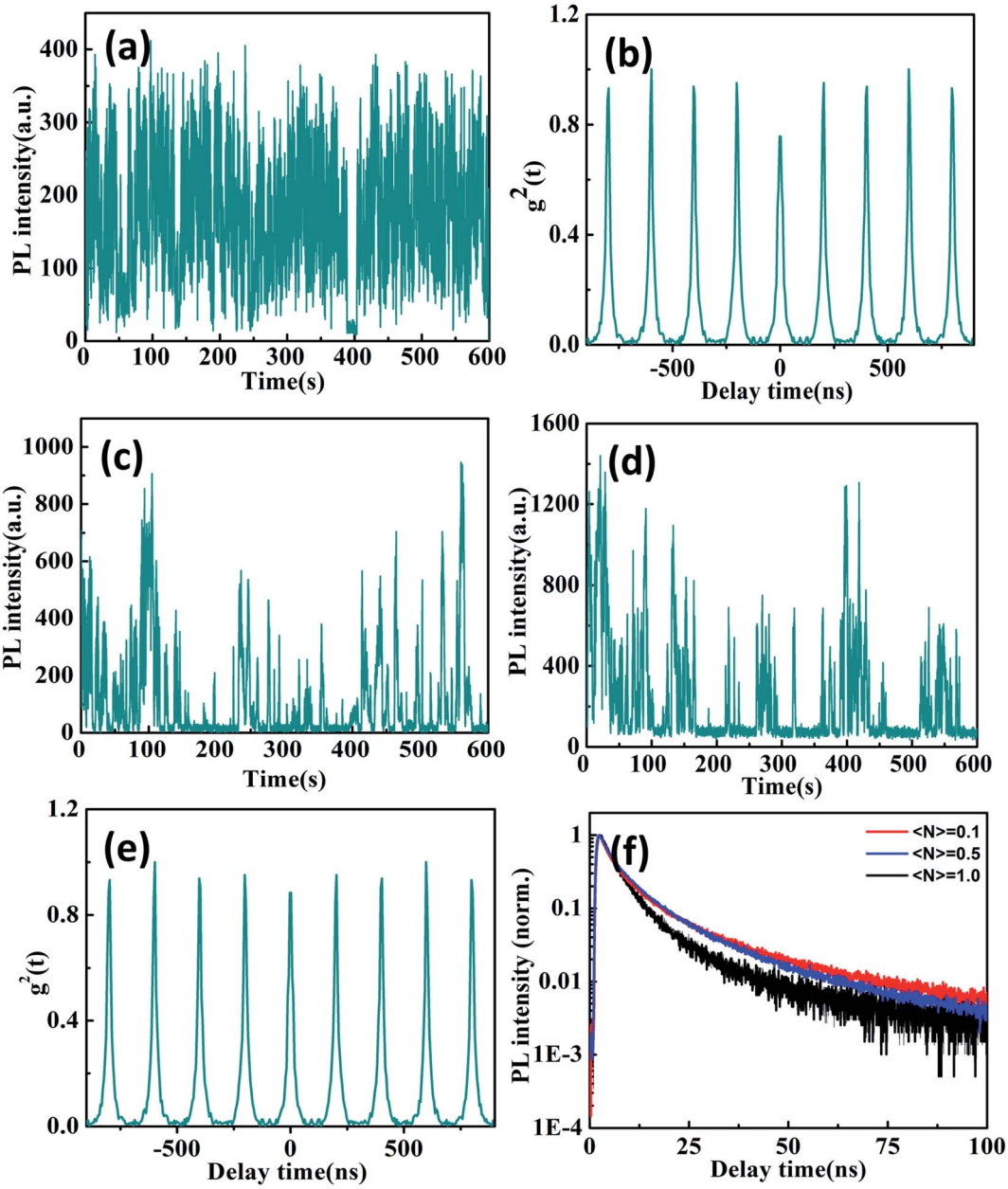

Fig. 5 Blinking trajectories of individual Cs_4PbBr_6 NC at low (a) $\sim\langle N\rangle = 0.1$ and high excitation level (c) $\sim\langle N\rangle = 0.5$, (d) $\sim\langle N\rangle = 1.0$, respectively. Antibunching functions $g^2(t)$ at low (b) $\sim\langle N\rangle = 0.1$ and high (e) $\sim\langle N\rangle = 1$ excitation levels. (f) Corresponding PL lifetimes at different excitation levels.

intensity bursts demonstrate dramatically similar lifetimes and the zero delay time second-order correlation function $g^2(0)$ is approximate ~1 as shown in Fig. 4b. Such behavior is very similar to that of Cs_4PbBr_6 NCs. These results thus confirm that the high efficiency PL emission of the $CsPbBr_3/Cs_4PbBr_6$ core/shell NCs is from the core of $CsPbBr_3$ NCs at lower excitation levels. However, it is clearly seen that the blinking behaviors of many $CsPbBr_3/Cs_4PbBr_6$ core/shell NCs initially demonstrate two-state emission and then are burst-like behaviors at higher excitation level. Thus, we can suggest that laser-induced structural reorganization in $CsPbBr_3/Cs_4PbBr_6$ core/shell NCs may lead to the formation of PL-active Br vacancy states at higher excitation level. Hence, these results confirm that $CsPbBr_3$ NCs encapsulated by Cs_4PbBr_6 shell structures exhibit different PL characteristics in comparison to pure $CsPbBr_3$ QDs.

Compared with the above $CsPbBr_3/Cs_4PbBr_6$ core/shell NCs, Fig. 5a presents the PL intensity trajectory of individual Cs_4PbBr_6 NCs at the $\langle N\rangle = 0.1$ excitation level. The PL intensity trajectory shows obvious noisiness behaviors that attribute to charge carrier recombination from the trap states located on the interior and surface of the Cs_4PbBr_6 NCs.[38] Because Br vacancies can act as a trap state and the trapping of electrons recombinate with holes, making the exciton recombination centers more efficient for green emission in Cs_4PbBr_6 NCs. We found that the majority of individual Cs_4PbBr_6 NCs still do not exhibit single photon properties with high $g^2(0)$ values at low excitation levels $\langle N\rangle = 0.1$ as shown in Fig. 5b. The PL lifetimes are fitted with bi-exponential functions with a short lifetimes of 2–3 ns and a long lifetimes of 11–13 ns as shown in Fig. 5f. The short and long components can be ascribed to the excitons located on the surface and interior of the Cs_4PbBr_6 NCs, respectively. Previous studies have shown that $CsPbBr_3$ NCs exhibit shorter PL lifetime compared to the Cs_4PbBr_6 NCs due to the presence of different deactivation pathways.[39,40]

As the excitation power further increases, the blinking behavior of Cs_4PbBr_6 NC visibly changes as shown in Fig. 5c and d. We observe a multitude intensity spikes that closely resemble the typical blinking behavior of individual molecular emitters. The PL intensity superlinearly increase due to the activation of more emissive centers in the Cs_4PbBr_6 NCs. Moreover, PL lifetimes extracted from different intensity bursts in the blinking trace are very close, suggesting their similar origins. Therefore, it has been proposed that intrinsic defect states within the band gap may serve as radiative recombination centers for the observed emission of Cs_4PbBr_6 NCs.[41,42]

4. Conclusions

In summary, $CsPbBr_3/Cs_4PbBr_6$ core/shell NCs were prepared and their PL properties were investigated at individual particle level. These results demonstrate that the Cs_4PbBr_6 shell with large band gap is helpful to confine the exciton and reach high PLQYs and high stability. The PL emission of $CsPbBr_3/Cs_4PbBr_6$ core/shell structures could be attributed to direct band-edge electron–hole radiative recombination in the $CsPbBr_3$ NCs, while the green emission (~2.4 eV) in Cs_4PbBr_6 originates from the exciton recombination at Br vacancy instead of a direct band-to-band transition. Therefore, the different carrier dynamics studies allow us to distinguish the origin of green emission between Cs_4PbBr_6 NCs and $CsPbBr_3$ NCs. The fundamental knowledge about interaction of excitons with interfaces in $CsPbBr_3/Cs_4PbBr_6$ core/shell NCs will provide new physical insights into the design and optimization of novel optoelectronics devices.

Author contributions

Q. F. Xu, S. F. Zhang, C. L. Yang conceived and planed the project. Y H. F. Ding, Y. S. Shan performed and analyzed the spectroscopy experiments. J. Z. Wang, J. Han, M. M. Jiao, K. J. Cao, H. F. Mu, M. L. Liu synthesized the materials. Q. F. Xu wrote the paper and discussed with other authors.

Conflicts of interest

The authors declare no competing financial interest.

Acknowledgements

The authors acknowledge the financial support of the Natural Science Foundation of China (No. 61905106), Shandong Province Natural Science Foundation (No. ZR2019MF057 and ZR2019MA066), Science and Technology Program of Shandong Province (J18KA222) and the Taishan Scholars Project of Shandong Province (tsqn201812098 and ts201511055).

References

1 T. Zhang, M. I. Dar, G. Li, F. Xu, N. Guo, M. Grätzel and Y. Zhao, *Sci. Adv.*, 2017, **3**, e1700841.
2 J. Y. Sun, F. T. Rabouw, X. F. Yang, X. Y. Huang, X. P. Jing, S. Ye and Q. Y. Zhang, *Adv. Funct. Mater.*, 2017, **27**, 1704371.
3 X. Li, F. Cao, D. Yu, J. Chen, Z. Sun, Y. Shen, Y. Zhu, L. Wang, Y. Wei, Y. Wu and H. Zeng, *Small*, 2017, **13**, 1603996.
4 B. A. Koscher, J. K. Swabeck, N. D. Bronstein and A. P. Alivisatos, *J. Am. Chem. Soc.*, 2017, **139**, 6566–6569.
5 A. Waleed, M. M. Tavakoli, L. Gu, Z. Wang, D. Zhang, A. Manikandan, Q. Zhang, R. Zhang, Y.-L. Chueh and Z. Fan, *Nano Lett.*, 2017, **17**, 523–530.
6 Z. K. Liu, Y. Bekenstein, X. C. Ye, S. C. Nguyen, J. Swabeck, D. D. Zhang, S. T. Lee, P. D. Yang, W. L. Ma and A. P. Alivisatos, *J. Am. Chem. Soc.*, 2017, **139**, 5309–5312.
7 J. Liang, C. Wang, Y. Wang, Z. Xu, Z. Lu, Y. Ma, H. Zhu, Y. Hu, C. Xiao, X. Yi, G. Zhu, H. Lv, L. Ma, T. Chen, Z. Tie, Z. Jin and J. Liu, *J. Am. Chem. Soc.*, 2017, **139**, 2852.
8 L. Protesescu, S. Yakunin, M. I. Bodnarchuk, F. Krieg, R. Caputo, C. H. Hendon, R. X. Yang, A. Walsh and M. V. Kovalenko, *Nano Lett.*, 2015, **15**, 3692–3696.
9 Y. Wang, Z. Chen, F. Deschler, X. Sun, T.-M. Lu, E. A. Wertz, J.-M. Hu and J. Shi, *ACS Nano*, 2017, **11**, 3355–3364.
10 A. Swarnkar, A. R. Marshall, E. M. Sanehira, B. D. Chernomordik, D. T. Moore, J. A. Christians, T. Chakrabarti and J. M. Luther, *Science*, 2016, **354**, 92–95.

11 W. Zhang, L. Peng, J. Liu, A. Tang, J.-S. Hu, J. Yao and Y. S. Zhao, *Adv. Mater.*, 2016, **28**, 4040–4046.
12 S. Yakunin, L. Protesescu, F. Krieg, M. I. Bodnarchuk, G. Nedelcu, M. Humer, G. De Luca, M. Fiebig, W. Heiss and M. V. Kovalenko, *Nat. Commun.*, 2015, **6**, 8056.
13 J. Pan, L. N. Quan, Y. Zhao, W. Peng, B. Murali, S. P. Sarmah, M. Yuan, L. Sinatra, N. M. Alyami, J. Liu, E. Yassitepe, Z. Yang, O. Voznyy, R. Comin, M. N. Hedhili, O. F. Mohammed, Z. H. Lu, D. H. Kim, E. H. Sargent and O. M. Bakr, *Adv. Mater.*, 2016, **28**, 8718–8725.
14 J. Song, J. Li, X. Li, L. Xu, Y. Dong and H. Zeng, *Adv. Mater.*, 2015, **27**, 7162–7167.
15 X. Li, Y. Wu, S. Zhang, B. Cai, Y. Gu, J. Song and H. Zeng, *Adv. Funct. Mater.*, 2016, **26**, 2435–2445.
16 X. Li, D. Yu, J. Chen, Y. Wang, F. Cao, Y. Wei, Y. Wu, L. Wang, Y. Zhu, Z. Sun, J. Ji, Y. Shen, H. Sun and H. Zeng, *ACS Nano*, 2017, **11**, 2015–2023.
17 H. Lu, W. Tian, F. Cao, Y. Ma, B. Gu and L. Li, *Adv. Funct. Mater.*, 2016, **26**, 1296–1302.
18 Y. Kim, E. Yassitepe, O. Voznyy, R. Comin, G. Walters, X. Gong, P. Kanjanaboos, A. F. Nogueira and E. H. Sargent, *ACS Appl. Mater. Interfaces*, 2015, **7**, 25007–25013.
19 D. Chen, G. Fang and X. Chen, *ACS Appl. Mater. Interfaces*, 2017, **9**, 40477–40487.
20 S. Ye, M. H. Yu, W. Yan, J. Song and J. L. Qu, *J. Mater. Chem. C*, 2017, **5**, 8187–8193.
21 W. Chen, J. Hao, W. Hu, Z. Zang, X. Tang, L. Fang, T. Niu and M. Zhou, *Small*, 2017, **13**, 1604085.
22 H. Hu, L. Wu, Y. Tan, Q. Zhong, M. Chen, Y. Qiu, D. Yang, B. Sun, Q. Zhang and Y. Yin, *J. Am. Chem. Soc.*, 2018, **140**, 406–412.
23 L. N. Quan, R. Quintero-Bermudez, O. Voznyy, G. Walters, A. Jain, J. Z. Fan, X. L. Zheng, Z. Y. Yang and E. H. Sargent, *Adv. Mater.*, 2017, **29**, 6.
24 Y. M. Chen, Y. Zhou, Q. Zhao, J. Y. Zhang, J. P. Ma, T. T. Xuan, S. Q. Guo, Z. J. Yong, J. Wang, Y. Kuroiwa, C. Moriyoshi and H. T. Sun, *ACS Appl. Mater. Interfaces*, 2018, **10**, 15905–15912.
25 Q. A. Akkerman, A. L. Abdelhady and L. Manna, *J. Phys. Chem. Lett.*, 2018, **9**, 2326–2337.
26 D. Han, H. L. Shi, W. M. Ming, C. K. Zhou, B. W. Ma, B. Saparov, Y. Z. Ma, S. Y. Chen and M. H. Du, *J. Mater. Chem. C*, 2018, **6**, 6398–6405.
27 Z. K. Liu, Y. Bekenstein, X. C. Ye, S. C. Nguyen, J. Swabeck, D. D. Zhang, S. T. Lee, P. D. Yang, W. L. Ma and A. P. Alivisatos, *J. Am. Chem. Soc.*, 2017, **139**, 5309–5312.
28 C. de Weerd, J. H. Lin, L. Gomez, Y. Fujiwara, K. Suenaga and T. Gregorkiewicz, *J. Phys. Chem.*, 2017, **121**, 19490–19496.
29 L. Yang, D. M. Li, C. Wang, W. Yao, H. Wang and K. X. Huang, *J. Nanopart. Res.*, 2017, **19**, 13.
30 J. M. Bao and V. G. Hadjiev, *Nano-Micro Lett.*, 2019, **11**, 18.
31 M. I. Saidaminov, J. Almutlaq, S. Sarmah, I. Dursun, A. A. Zhumekenov, R. Begum, J. Pan, N. Cho, O. F. Mohammed and O. M. Bakr, *ACS Energy Lett.*, 2016, **1**, 840–845.
32 J. Yin, H. Yang, K. Song, A. M. El-Zohry, Y. Han, O. M. Bakr, J. L. Bredas and O. F. Mohammed, *J. Phys. Chem. Lett.*, 2018, **9**, 5490–5495.
33 J. Yin, Y. H. Zhang, A. Bruno, C. Soci, O. M. Bakr, J. L. Bredas and O. F. Mohammed, *ACS Energy Lett.*, 2017, **2**, 2805–2811.
34 J. H. Cha, J. H. Han, W. Yin, C. Park, Y. Park, T. K. Ahn, J. H. Cho and D. Y. Jung, *J. Phys. Chem. Lett.*, 2017, **8**, 565–570.
35 S. Seth and A. Samanta, *J. Phys. Chem. Lett.*, 2017, **8**, 4461–4467.
36 X. Chen, D. Q. Chen, J. N. Li, G. L. Fang, H. C. Sheng and J. S. Zhong, *Dalton Trans.*, 2018, **47**, 5670–5678.
37 Q. A. Akkerman, S. Park, E. Radicchi, F. Nunzi, E. Mosconi, F. De Angelis, R. Brescia, P. Rastogi, M. Prato and L. Manna, *Nano Lett.*, 2017, **17**, 1924.
38 Y. Zhang, T. Guo, H. Yang, R. Bose, L. Liu, J. Yin, Y. Han, O. M. Bakr, O. F. Mohammed and A. V. Malko, *Nat. Commun.*, 2019, **10**, 2930.
39 A. A. Cordones and S. R. Leone, *Chem. Soc. Rev.*, 2013, **42**, 3209.
40 N. Yarita, H. Tahara, T. Ihara, T. Kawawaki, R. Sato, M. Saruyama, T. Teranishi and Y. Kanemitsu, *J. Phys. Chem. Lett.*, 2017, **8**, 1413.
41 Y. Zhang, T. Guo, H. Yang, R. Bose, L. Liu, J. Yin, Y. Han, O. M. Bakr, O. F. Mohammed and A. V. Malko, *Nat. Commun.*, 2019, **10**, 2930.
42 J. Yin, P. Maity, M. De Bastiani, I. Dursun, O. M. Bakr, J. L. Bredas and O. F. Mohammed, *Sci. Adv.*, 2017, **3**, 1701793.